Heterogeneity in PFC-amygdala connectivity in middle childhood, and concurrent interrelations with inhibitory control and anxiety symptoms☆

Kelley E. Gunther [*], Daniel Petrie, Alaina L. Pearce, Bari A. Fuchs, Koraly Pérez-Edgar, Kathleen L. Keller, Charles Geier

Penn State University, United States

ABSTRACT

The prefrontal cortex (PFC) is a key brain area in considering adaptive regulatory behaviors. This includes regulatory projections to regions of the limbic system such as the amygdala, where the nature of functional connections may confer lower risk for anxiety disorders. The PFC is also associated with behaviors like executive functioning. Inhibitory control is a behavior encompassed by executive functioning and is generally viewed favorably for adaptive socioemotional development. Yet, some research suggests that high levels of inhibitory control may actually be a risk factor for some maladaptive developmental outcomes, like anxiety disorders. In a sample of 51 children ranging from 7 to 9 years old, we examined resting state functional connectivity between regions of the PFC and the amygdala. We used Subgrouping Group Iterative Multiple Model Estimation (S-GIMME) to identify and characterize data-driven subgroups of individuals with similar networks of connectivity between these brain regions. Generated subgroups were collapsed into children characterized by the presence or absence of recovered connections between the PFC and amygdala. For subsets of children with available data (N = 38–44), we then tested whether inhibitory control, as measured by a stop signal task, moderated the relation between these subgroups and child-reported anxiety symptoms. We found an inverse relation between stop-signal reaction times and reported count of anxiety symptoms when covarying for connectivity group, suggesting that greater inhibitory control was actually related to greater anxiety symptoms, but only when accounting for patterns of PFC-amygdala connectivity. These data suggest that there is a great deal of heterogeneity in the nature of functional connections between the PFC and amygdala during this stage of development. The findings also provide support for the notion of high levels of inhibitory control as a risk factor for anxiety, but trait-level biopsychosocial factors may be important to consider in assessing the nature of risk.

The prefrontal cortex (PFC) is broadly associated with a wide spectrum of regulatory tasks, including executive functioning and emotion regulation (Miller and Cohen, 2001). Conventionally, the ability to regulate one's behavior is viewed as a mechanism for adaptive development, often understood as a positive relation between emotion regulation and positive outcomes such as school success (Graziano et al., 2007) and lower rates of some psychopathologies (Cole and Deater-Deckard, 2009), such that "more is better". However, recent data suggest that it may be possible to have too much of a good thing as higher levels of inhibitory control, a sub-domain of executive functioning, may actually exacerbate risk for anxiety disorders (Carlson and Wang, 2007; Eggum-Wilkens et al., 2016; Henderson et al., 2015; Henderson and Wilson, 2017; Thorell et al., 2004; White et al., 2011). While it is difficult to quantify the exact prevalence, it is estimated that up to 28.3% of individuals worldwide are affected by anxiety disorders (Baxter et al., 2013), with an even larger portion impacted by symptoms below clinical threshold. Anxiety disorders also come at a great cost to the individual as well as society, as they are linked to a number of negative societal and individual outcomes, including diminished productivity in the workplace and greater use of healthcare services (Hoffman et al., 2008; Wittchen, 2002). Moreover, onset of symptoms often occurs in childhood (Beesdo et al., 2009). Thus, it is important to

better understand the etiology of anxiety disorders, as well as mechanisms of risk and resilience through development.

To better characterize the complex association between inhibitory control and risk for anxiety, it is critical to better understand the neurological processes that contribute to risk for anxiety. Functional connections between the PFC and the amygdala, a limbic structure associated with the detection of emotionally salient stimuli, are associated with adaptive socioemotional development. For example, negative resting state functional connectivity between these structures is associated with fewer anxiety symptoms (Gee et al., 2013; Tottenham and Gabard-Durnam, 2017). With circuits between the PFC and amygdala captured as a marker of trait-level regulation, we asked whether these patterns may help explain the idiosyncratic or inconsistent relations between executive functioning behaviors and anxiety symptoms seen in the literature. As such, we tested whether the interaction between inhibitory control performance and resting state connections between regions of the amygdala and the PFC related to anxiety symptomology in a cross-sectional sample of school-age children.

1. Executive functioning

Executive functioning allows an individual to flexibly respond to stimuli even in the face of a competing prepotent response, supporting goal attainment (Diamond, 2006). Executive functioning is closely tied to the functioning of the PFC (Zelazo et al., 2008). The PFC, in turn, has a protracted developmental trajectory, not reaching maturity until young adulthood (Casey et al., 2005). As such, adult-like proficiency in executive functioning has a delayed emergence relative to many other domains of development (Welsh et al., 1991). For the purposes of this manuscript, we consider EF through the lens of a three-factor model, dividing the broad umbrella term into the dissociable components of set shifting, working memory/updating, and inhibitory control (Miyake et al., 2000). Specifically, inhibitory control refers to the ability to withhold a dominant response in favor of a subdominant one even in the presence of distractions, set shifting refers to the ability to flexibly toggle between rule sets, perspectives, or loci of attention, and working memory updating refers to the ability to not only hold information in one's mind, but to update as information changes (Diamond, 2006; Miyake et al., 2000). However, these subdomains of executive functioning are not necessarily a unitary construct. High levels of performance in one domain (i.e., set shifting) need not confer high levels of performance in another (i.e., inhibitory control; Blackwell et al., 2014).

Positive developmental outcomes typically associated with higher levels of executive functioning include increased school readiness (Fitzpatrick et al., 2014) and more sophisticated theory of mind (Carlson and Moses, 2001) relative to peers. Impaired executive functioning is thought to be a transdiagnostic risk factor for a wide variety of clinical diagnoses (Snyder et al., 2015; Zelazo, 2020), including Attention Deficit Hyperactivity Disorder (ADHD; e.g. Barkley, 1997), Obsessive Compulsive Disorder (OCD; e.g. Shin et al., 2014) and bipolar disorder (i.e. Bora et al., 2009). Increased levels of attention shifting may operate as a protective mechanism against anxiety (Eggum-Wilkens et al., 2016; Henderson et al., 2015; Henderson and Wilson, 2017; Toren et al., 2000; White et al., 2011). Similar findings have been reported for working memory (Basten et al., 2012; Moran, 2016). However, research remains mixed on whether inhibitory control acts in the same protective fashion.

Supporting the traditional hypothesis that "more is better," some work finds an inverse relation between inhibitory control and anxiety symptoms in both children (Kooijmans et al., 2000; Lengua, 2003; Wolfe and Bell, 2014) and adults (Ansari and Derakshan, 2011; Basten et al., 2011). However, other research has found that increased inhibitory control may act as a risk factor for higher levels of anxiety, particularly among children (Carlson and Wang, 2007; Eggum-Wilkens et al., 2016). Moreover, a body of work has found that inhibitory control may interact with behaviors associated with trait-level regulation such as social fear (Brooker et al., 2016), negative emotionality (Rodrigues et al., 2021), or

behavioral inhibition (Henderson et al., 2015; Henderson and Wilson, 2017; White et al., 2011) to predict anxiety in development. As such, while under control may relate to maladaptive developmental outcomes (Ansari and Derakshan, 2011; Basten et al., 2011; Kooijmans et al., 2000; Lengua, 2003; Wolfe and Bell, 2014), overcontrol may also be similarly deleterious (Carlson and Wang, 2007; Eggum-Wilkens et al., 2016; Henderson et al., 2015; Henderson and Wilson, 2017). Thus, the relation between inhibitory control and anxiety symptoms may be U-shaped rather than linear. That is, both lower and higher levels of inhibitory control may relate to greater anxiety symptoms, and the optimal range of inhibitory control may instead be found at more moderate levels (Gunther and Pérez-Edgar, 2021; Northoff and Tumati, 2019).

A proposed mechanism underlying the possible U-shaped association between inhibitory control and anxiety symptoms is that high levels of inhibitory control contribute to behavioral rigidity and overcontrol (Gunther and Pérez-Edgar, 2021; Henderson et al., 2015; Henderson and Wilson, 2017). Overcontrolled tendencies may potentiate maladaptive social behaviors, which may in turn promote negative affect, limit environmental engagement and learning, and ultimately increase risk for psychopathology (Gunther and Pérez-Edgar, 2021; Henderson et al., 2015; Henderson and Wilson, 2017). More work is needed to characterize and understand these relations and underlying mechanisms.

2. The PFC, functional connections to the amygdala, and emotion regulation

The amygdala is often considered a "salience detector," responding to stimuli important for adaptive engagement with one's environment (e.g., affective stimuli; Adolphs, 2008). Considering the regulatory role of the PFC (Zelazo et al., 2008), neural circuitry between the PFC and the amygdala is critical for adaptive socioemotional processes (Ochsner et al., 2012). Functional connections between the amygdala and the PFC evolve over the course of development and throughout young adulthood (Taber-Thomas and Pérez-Edgar, 2015). Indeed, the PFC develops on an extremely protracted timeline, not reaching maturity until young adulthood (Casey et al., 2005). Meanwhile, the amygdala reaches near-maturity in early childhood (Gabard-Durnam et al., 2018; Saygin et al., 2015). This temporal order of development suggests that while amygdala function is shaped early in life by environmental influences, the activity of the amygdala both influences the development of the PFC and shapes the nature of functional connections between the amygdala and PFC (Tottenham and Gabard-Durnam, 2017). Animal work suggests that functional connections from the amygdala to the PFC emerge prior to the reciprocal connections, demonstrating this directional cascade in development (Bouwmeester et al., 2002a; 2002b; Tottenham and Gabard-Durnam, 2017). Thus, the PFC itself, as well as its circuitry to the amygdala, are in flux through development and are integral to consider in assessing adaptive socioemotional development.

Resting state connectivity analyses aim to assess functional connections in the brain, in the absence of a task (Uddin et al., 2010). Resting state data provide unique information regarding brain networks and circuits, highlighting spontaneous activity in these circuits rather than activity elicited by a task (Lv et al., 2018; Uddin et al., 2010). However, resting state measures have been relatively under-utilized in this area of research. Here, we review findings pertaining to functional connections between the amygdala and PFC. We note that the majority of published work examining connectivity between the PFC and amygdala is either task-elicited rather than examining networks at rest, and/or predominantly conducted in adult samples.

Gee et al. (2013) found in a healthy cross-sectional sample of children that the functional connectivity between the PFC and the amygdala in response to fearful faces flips in magnitude from positive to negative around 10 years of age. Corresponding with this finding, there were also age-related decreases in amygdala activity in response to fearful faces through childhood. These findings suggest that changes in

fronto-amygdala connectivity may relate to the downregulation of the amygdala in response to fearful stimuli by dampening amygdala reactivity (Gee et al., 2013). Additionally, the magnitude of the connection between the amygdala and the medial prefrontal cortex (mPFC) significantly mediated the association between age and reported separation anxiety within the sample. Furthermore, when covarying for age, children with negative connectivity were more likely to have lower reported anxiety (Gee et al., 2013). Therefore, these age-related changes in task-based fronto-amygdala connectivity and negative fronto-amygdala connectivity may be critical in adaptive socioemotional development.

Findings are mixed when identifying patterns of resting state connectivity that characterize anxious individuals. Some work finds no significant differences in resting state connectivity between regions of the PFC and the amygdala as a function of anxiety (Prater et al., 2013). However, Hahn et al. (2011) found that clinically anxious adults may have decreased resting state connectivity between the left orbitofrontal cortex and the left amygdala compared to healthy controls, suggesting that less robust functional connections between these regions may be related to greater anxious symptomatology. Similarly, Liu et al. (2015) found that adolescents with a generalized anxiety disorder diagnosis showed decreased connectivity between the left amygdala and left dorsolateral prefrontal cortex (dlPFC) at rest.

On the other hand, Geiger et al. (2016) reported that socially anxious adults showed *increased* connectivity between the left orbitofrontal gyrus and the left amygdala. They also examined the executive control network, a network of brain regions including both cortical (e.g. fronto-parietal regions, middle temporal gyrus, insula, cingulate gyrus, and inferior parietal lobe) and subcortical (e.g. cerebellum) structures and associated with goal-oriented behavior. Within the left executive control network, the authors found increased connectivity within the left middle frontal gyrus and decreased connectivity within the left orbitofrontal gyrus. The authors suggest that the high levels of connectivity found in fronto-amygdala circuits paired with low levels of connectivity in the executive control network may be capturing an imbalance between top-down and bottom-up control as part of the etiology of anxious symptomatology. Taken together, more work is needed to more thoroughly characterize patterns of resting state connectivity that may confer risk for anxiety, especially in childhood.

3. Assessing resting state connectivity using GIMME

Traditional network connectivity approaches (e.g., correlation-based), while valuable, are not able to determine directionality between brain regions of interest (ROIs; Smith et al., 2011). Group Iterative Multiple Model Estimation (GIMME), in contrast, is a statistical approach that reliably calculates direction of influence between ROIs on both an individual and group level (Gates and Molenaar, 2012; Gates et al., 2014; Smith et al., 2011). The ability to consider the directionality of connections will help to elucidate any potential upregulatory or downregulatory connections from PFC to amygdala. Additionally, while traditional resting-state analytic approaches rely on the assumption of group homogeneity, GIMME accommodates heterogeneity in connectivity across individuals in the sample (Gates and Molenaar, 2012; Gates et al., 2014). Eliminating the assumption of homogeneity may be more appropriate in examining functional connectivity during a resting state scan, which is less constrained.

GIMME also takes a person-centered approach in assessing network connectivity. In traditional network approaches, which are not person-centered, the map of nodes/edges that is derived represents averages for the population but may not actually apply to or describe any one individual in the sample (Molenaar, 2004; Molenaar and Campbell, 2009). A person-centered approach, first building a model for each individual, is a solution to this problem (Gates and Molenaar, 2012).

Secondarily, GIMME uses both contemporaneous and lagged relations in networking mapping, where traditional correlation approaches do not consider lagged relations. Considering lagged relations establishes Granger causality as well as decreases false positives (Gates and Molenaar, 2012).

Finally, GIMME is an alternative to brain-wide associations, or examining associations between brain region correlations and a behavioral phenotype, which a recent publication suggests lacks power and thus replicability (Marek et al., 2022). By using time series data to derive network maps between ROIs on an individual level, that were then used to form data-driven subgroups, we are using a metric that may very well be orthogonal to traditional rsFC strength, and we believe may be more robust especially in light of these recent publications.

GIMME also has subgrouping functionality ("S-GIMME"), which generates subgroups of individuals based on similarities in individual-level functional connectivity maps (Gates et al., 2017). This data-driven method allows for the identification and characterization of neural heterogeneity into categorical subgroups independent of behavioral phenotypes. For example, by applying S-GIMME to resting state data from a sample of children with and without ADHD, Gates et al. (2014) identified 5 subgroups of children with unique connectivity patterns amongst fronto-parietal ROIs. Two of the subgroups were composed overwhelmingly of children with an ADHD diagnosis. This suggests both heterogeneity amongst children with ADHD, but also a distinctiveness in connectivity patterns of children with ADHD versus typically developing children. These findings also suggest that using a data-driven grouping approach may provide a more nuanced way of characterizing populations above and beyond a clinical diagnosis (Gates et al., 2014).

Similarly, McCormick et al. (2019) collected functional magnetic resonance imaging (fMRI) data during the Balloon Analogue Risk Task (BART; Lejuez et al., 2002) to assess risky decision-making in a sample of both children and adults. They found that the subgroups generated by S-GIMME using cortical and subcortical ROIs were different from the *a priori* adolescent, young adult, and adult groups. Moreover, data-derived and *a priori* groups were differentiated by distinct patterns of connections between ROIs during the task (McCormick et al., 2019). These papers suggest that S-GIMME may provide additional nuance in understanding profiles of risk above and beyond categorical variables conventionally used to describe a sample (Gates et al., 2014; McCormick et al., 2019). Thus, this grouping feature of GIMME will help us identify subgroups based on neural patterns, regardless of overt behavior, to test as a potential risk or protective factor for anxiety.

4. Present study

In the present study we examined if inhibitory control proficiency moderated the association between resting state PFC-amygdala connectivity and anxiety symptoms in 7-9-year-old children. Based on the reviewed literature, this stage of childhood may be just prior to a developmental shift from positive to negative connectivity between PFC and amygdala that has been observed around age 10 (Gee et al., 2013). The time preceding this developmental shift can be inferred to be marked by rapid developmental change, especially as newly-emerging executive skills begin to stabilize. Thus, this stage of childhood is considered a critical window in which to examine individual differences in connectivity, especially as these differences may pertain to anxiety (Pérez-Edgar et al., 2020).

We first characterized patterns of resting state PFC-amygdala connectivity in a sample of children 7–9 years of age using S-GIMME, an emerging method of generating data-driven subgroups of connectivity patterns (Gates et al., 2017). Due to the relative novelty of this method, we first sought to describe these subgroups and examine how these connectivity patterns related to both inhibitory control performance and child-reported anxiety symptoms. Then, we tested whether inhibitory control proficiency, a potential risk factor for anxiety, moderated the association between PFC-amygdala connectivity and anxiety symptoms in middle childhood.

Although current work has produced inconsistent findings on the

relation between functional connectivity and symptoms of anxiety (Geiger et al., 2016; Hahn et al., 2011; Liu et al., 2015; Prater et al., 2013), we predicted that children with no recovered connections between regions of the PFC and the amygdala will report greater levels of anxiety. Conversely, we posit that children with more dense patterns of recovered connections between the PFC and the amygdala will report lower levels of anxiety. We also predicted that children with recovered connections between regions of the PFC and the amygdala would display better performance on our measure of inhibitory control, the stop signal task. Finally, we predicted that inhibitory control performance will moderate the relation between connectivity group and reported anxiety symptoms, where higher levels of inhibitory control will strengthen the relation between weak/negative PFC-amygdala connectivity and greater anxiety symptoms. In other words, children without recovered resting state connections between the PFC and the amygdala, which may confer lower levels of regulation, will be more likely to show higher levels of reported anxiety if they also show higher levels of inhibitory control.

5. Methods

5.1. Participants

At time of data analysis, 77 children were enrolled in an ongoing longitudinal, family-risk study originally designed to examine the neurocognitive determinants of pediatric obesity. The study consisted of six separate laboratory visits. Data included in this study were acquired across two different visits detailed below.

Based on the family risk design used in the ongoing study, all children were healthy weight at enrollment (BMI-for-age < 85th %), but were either "high risk" for obesity if both biological parents had BMIs in the overweight (i.e., father >25 kg/m^2) or obese (i.e., mother >30 kg/m^2) range or "low risk" if both biological parents had BMIs in the healthy weight range (<25 kg/m^2). Participants were excluded if they had any neurodevelopmental disorders, colorblindness, claustrophobia, contraindications for fMRI, did not speak English as a first language, if they were on any medications/had any medical diagnoses that may impact the child's appetite or food preferences/choices, were not of healthy body weight (body mass index for age % < 85), or if their parents did not meet the BMI criteria for high or low risk.

Of the enrolled participants, 65 completed a resting state fMRI scan. However, 12 children's scans could not be used due to errors in file writing that prevented the preprocessing pipeline to run to completion, and one participant was excluded for a diagnosis of ADHD after initial enrollment in the ongoing study. No exclusions were made for excessive motion; we set the criteria that a participant would be excluded if over 50% of volumes exceeded the motion threshold and no participants were over this value ($M = 0.12$, $SD = 0.12$). The average root mean squared head position change for the entire sample was 0.25 ($SD = 0.23$). The final sample included 51 children ranging from 7 to 9 years of age at the time of the fMRI ($M = 8.13$, $SD = 0.60$), but children were between 7 and 8 years old at time of recruitment. The modal family income was over $100,000 USD. 76.5% of parents who filled out questionnaires had a Bachelor's degree or higher, and 68.6% of their partners had a Bachelor's degree or higher. Full details of the sample are described in Table 1. These demographics reflect the surrounding rural college town community (U.S. Census Bureau, 2021). All study procedures were approved by the Institutional Review Board at the Pennsylvania State University. All parents and children completed written consent/assent and were compensated for their time.

5.2. Protocol

Data included in this study were collected at visits two and six. State anxiety measurements were collected on visit two following a laboratory meal, while fMRI data and stop signal task were collected on visit six. For visit six, children were instructed to fast 3 h prior to arrival, and once

Table 1
Table describing demographics of the final sample.

	N	%
Sex (female)	30	58.8
Familial obesity risk status (high risk)	19	37.3
Race		
White	49	96.1
Asian	2	3.9
Ethnicity		
Not Hispanic or Latino	52	100
Yearly income		
$20,000 - $35,999	2	3.9
$36,000 - $50,999	5	9.8
$51,000 - $75,999	12	23.5
$76,000 - $100,000	11	21.6
Over $100,000	19	37.3
Declined to respond	2	3.9
Primary parent education		
High School or GED	7	13.7
Associate's Degree	4	7.8
Bachelor's Degree	21	40.2
Master's Degree	11	21.6
Ph.D.	8	15.7
Parent's partner's education		
High School or GED	8	15.7
Associate's Degree	1	2.0
Tech or Vocational School	5	9.8
Bachelor's Degree	18	35.3
Master's Degree	10	19.6
J.D.	1	1.9
M.D.	1	1.9
Ph.D.	5	9.8
Other/did not respond	2	3.9
	Mean	SD	Range
Age at scan	8.13 years	0.60	7.14–9.26

they arrived, rated their fullness using a child-appropriate visual analog scale (VAS; Keller et al., 2006). If children were <25% full according to the VAS, they were given a small snack (apple juice and granola bar) so that they were in a neutral appetitive state during the fMRI. Before and after the scan, children rated their state anxiety using the Children's Anxiety Meter – State (CAMS-S; Ersig et al., 2013). Following the fMRI, children completed a delay of gratification task, were offered a small snack (grapes, apple juice, cheese crackers), and rated images they saw in the scanner prior to completing the stop signal task.

In preparation for the fMRI, children completed a two-session mock scanner protocol at visits four and five. As part of this protocol, children were able to explore the mock scanner, enter the bore, play a game on the computer screen, and complete movement training games. This training protocol has resulted in high success rates (i.e., >90% useable functional scans) in prior studies with this age-group (Adise et al., 2018; English et al., 2019).

5.3. Data acquisition

Imaging data were acquired using a 3-T MRI scanner (MAGNETOM Trio with Tim system, Siemens Medical Solutions, Erlangen, Germany). High resolution structural images were collected using a T1-weighted magnetization-prepared rapid acquisition gradient echo (MPRAGE) sequence to acquire 160 slices (1 × 1x1mm voxels). During this scan, children watched a video of baby animals to improve scan quality and reduce motion.

Immediately following the anatomical scan, resting state data were collected. During the resting state scan, children watched an abstract video. While a screen with a fixation cross is perhaps the most common protocol for resting state data acquisition, recent work suggests that this specific visual stimulus improved task compliance and decreased motion artifacts while retaining resting state "task" integrity (Vanderwal et al., 2015). Resting state functional images were collected using a

T2*-weighted gradient single-shot blood-oxygen-level-dependent (BOLD) echo planar imaging (EPI) sequence to acquire 33 slices (3 × 3x3mm voxels, TR = 2000 ms, TE = 26.0 ms, flip angle = 90, FoV = 220 × 220, slice gap = 0 mm). The resting state scan was 6 min long (180 vol, TR = 2000 ms). Both the anatomical scan and the resting state were the first two scans of a larger protocol that involved assessing children's responses to food images and office supplies. These data will be published in a forthcoming submission.

5.4. Data preprocessing

fMRIprep. Results included in this manuscript come from pre-processing performed using fMRIPrep 20.2.1 (Esteban et al., 2018a, 2018b; Esteban et al., 2018a, 2018b; RRID:SCR_016216), which is based on Nipype 1.5.1 (Gorgolewski et al., 2011; RRID:SCR_002502).

T1-weighted (T1w) images were corrected for intensity non-uniformity (INU) with N4BiasFieldCorrection (Tustison et al., 2010), distributed with ANTs 2.3.3 (Avants et al., 2008, RRID:SCR_004757), and used as T1w-reference throughout the workflow. The T1w-reference was then skull-stripped with a Nipype implementation of the ants-BrainExtraction.sh workflow (from ANTs), using OASIS30ANTs as target template. Brain tissue segmentation of cerebrospinal fluid (CSF), white-matter (WM) and gray-matter (GM) was performed on the brain-extracted T1w using fast (FSL 5.0.9, RRID:SCR_002823, Zhang et al., 2001). Volume-based spatial normalization to one standard space (MNI152NLin2009cAsym) was performed through nonlinear registration with antsRegistration (ANTs 2.3.3), using brain-extracted versions of both T1w reference and the T1w template. The following template was selected for spatial normalization: ICBM 152 Nonlinear Asymmetrical template version 2009c (Fonov et al., 2009), RRID:SCR_008796; Template Flow ID: MNI152NLin2009cAsym], For BOLD runs collected during resting state, the following preprocessing was performed. First, a reference volume and its skull-stripped version were generated using a custom methodology of fMRIPrep. A deformation field to correct for susceptibility distortions was estimated based on fMRIPrep\u2019s fieldmap-less approach. The deformation field is that resulting from co-registering the BOLD reference to the same-subject T1w-reference with its intensity inverted (Huntenburg, 2014; Wang et al., 2017). Registration is performed with antsRegistration (ANTs 2.3.3), and the process regularized by constraining deformation to be nonzero only along the phase-encoding direction and modulated with an average fieldmap template (Treiber et al., 2016). Based on the estimated susceptibility distortion, a corrected EPI (echo-planar imaging) reference was calculated for a more accurate co-registration with the anatomical reference. The BOLD reference was then co-registered to the T1w reference using flirt (FSL 5.0.9, Jenkinson and Smith, 2001) with the boundary-based registration (Greve and Fischl, 2009) cost-function.

Co-registration was configured with nine degrees of freedom to account for distortions remaining in the BOLD reference. Head-motion parameters with respect to the BOLD reference (transformation matrices, and six corresponding rotation and translation parameters) are estimated before any spatiotemporal filtering using mcflirt (FSL 5.0.9, Jenkinson et al., 2002). BOLD runs were slice-time corrected using 3dTshift from AFNI 20160207 (Cox and Hyde, 1997, RRID: SCR_005927). The BOLD time-series (including slice-timing correction when applied) were resampled onto their original, native space by applying a single, composite transform to correct for head-motion and susceptibility distortions. These resampled BOLD time-series will be referred to as preprocessed BOLD in original space, or just preprocessed BOLD. The BOLD time-series were resampled into standard space, generating a preprocessed BOLD run in MNI152NLin2009cAsym space.

First, a reference volume and its skull-stripped version were generated using a custom methodology of fMRIPrep (Esteban et al., 2018a, 2018b, supplementary note 3). Several confounding time-series were calculated based on the preprocessed BOLD: framewise displacement (FD), DVARS and three region-wise global signals. FD was computed using two formulations following Power (absolute sum of relative motions; Power et al., 2014) and Jenkinson (relative root mean square displacement between affines; Jenkinson et al., 2002). FD and DVARS are calculated for each functional run, both using their implementations in Nipype (following the definitions by Power et al., 2014). The three global signals are extracted within the CSF, the WM, and the whole-brain masks.

Additionally, a set of physiological regressors were extracted to allow for component-based noise correction (CompCor, Behzadi et al., 2007). Principal components are estimated after high-pass filtering the preprocessed BOLD time-series (using a discrete cosine filter with 128s cut-off) for the two CompCor variants: temporal (tCompCor) and anatomical (aCompCor). tCompCor components are then calculated from the top 2% variable voxels within the brain mask. For aCompCor, three probabilistic masks (CSF, WM and combined CSF + WM) are generated in anatomical space. The implementation differs from that of Behzadi et al. in that instead of eroding the masks by 2 pixels on BOLD space, the aCompCor masks are subtracted a mask of pixels that likely contain a volume fraction of GM. This mask is obtained by thresholding the corresponding partial volume map at 0.05, and it ensures components are not extracted from voxels containing a minimal fraction of GM.

Finally, these masks are resampled into BOLD space and binarized by thresholding at 0.99 (as in the original implementation). Components are also calculated separately within the WM and CSF masks. For each CompCor decomposition, the k components with the largest singular values are retained, such that the retained components\u2019 time series are sufficient to explain 50 percent of variance across the nuisance mask (CSF, WM, combined, or temporal). The remaining components are dropped from consideration.

The head-motion estimates calculated in the correction step were also placed within the corresponding confounds file. The confound time series derived from head motion estimates and global signals were expanded with the inclusion of temporal derivatives and quadratic terms for each (Satterthwaite et al., 2013). Frames that exceeded a threshold of 0.5 mm FD or 1.5 standardized DVARS were annotated as motion outliers. All resamplings can be performed with a single interpolation step by composing all the pertinent transformations (i.e., head-motion transform matrices, susceptibility distortion correction when available, and co-registrations to anatomical and output spaces). Gridded (volumetric) resamplings were performed using antsApplyTransforms (ANTs), configured with Lanczos interpolation to minimize the smoothing effects of other kernels (Lanczos, 1964). Non-gridded (surface) resamplings were performed using mri_vol2surf (FreeSurfer).

Many internal operations of fMRIPrep use Nilearn 0.6.2 (Abraham et al., 2014, RRID:SCR_001362), mostly within the functional processing workflow. More details of the pipeline can be seen the section corresponding to workflows in fMRIPrep documentation.

XCP Engine. XCP Engine cleans and parses time series data from the preprocessed fMRIprep data. In this processing, we selected the 36P + DESPIKE to clean for motion artifacts (Lydon-Staley et al., 2019). From XCP Engine, we derived time series data for each of our ROIs. For our analysis we *a priori* selected bilateral ROIs encompassed by the PFC, which was central to our hypothesis: the frontal pole, frontal medial cortex, frontal orbital cortex, and the amygdala. ROIs were anatomically defined by the Harvard Oxford atlas, used in prior studies of similar age range and brain areas of interest (i.e., Liu et al., 2021).

5.5. Resting state connectivity

GIMME was used to construct functional connectivity maps during resting state fMRI (Gates and Molenaar, 2012; Gates et al., 2014; Smith et al., 2011). GIMME operates within a unified structural equation model framework (uSEM; Gates et al., 2010; Kim et al., 2007), where a data-driven algorithm constructs functional connectivity maps by using information from both the individual- and group-level through a process of model building and model pruning. First, information is pooled across

all participants and used to create a connectivity map that is representative of the sample using modification indices (Sörbom, 1989). Group paths are retained if they improve model fit, according to modification indices, at a user-defined cutoff value. Following recommendations from Gates et al. (2021), we lowered the default group level threshold from the default 75%–51%. This reflects criteria specifying that greater than half of individuals must have a path present and improve overall model fit for the path to be represented in the group level map.

Importantly, all autoregressive paths are freely estimated in order to determine directionality between ROI paths by establishing Granger causality (Granger, 1969; Lane and Gates, 2017). The group map is then pruned by eliminating paths which, because of adding paths across iterations, no longer improve model fit. Next, individual-level paths are estimated. For each individual, the group-level model is fit, and then modification indices are used to assess whether additional paths for each individual would improve the fit of the model. This iterative procedure continues until excellent model fit is obtained. Excellent model fit is defined as exceeding two out of four fit indices (Gates and Molenaar, 2012): root mean squared of approximation (RMSEA) $\leq$ 0.05; standardized root mean residual (SRMR) $\leq$ 0.05; comparative fit index (CFI) $\geq$ 0.95; non-normed fit index (NNFI) $\geq$ 0.95.

We allowed GIMME to freely construct subgroups based on individual connectivity maps. With this approach, the researcher does not need to specify the number of subgroups. Rather, the best fit for number of subgroups is chosen by the algorithm (Gates et al., 2017; McCormick et al., 2019). S-GIMME decides the number of subgroups by creating a similarity matrix using the individual estimates of the group-level connections (Gates et al., 2017). Then, the similarity matrix is subjected to the Walktrap community detection approach (Pons and Latapy, 2006), which arrives at subgroups by utilizing data-driven random walks to maximize modularity. Thus, subgroups are based on the characteristics of the individual-level connectivity maps. Walktrap approaches have been shown to avoid spurious subgroupings and do not rely on significance testing which is a common problem in network contexts (Gates et al., 2017). After S-GIMME identifies distinct subgroups, unique subgroup specific paths are identified in a similar way as the group- and individual-level paths. We retained the default 50% as the subgroup level cutoff, reflecting criteria specifying that half of the individuals within a designated subgroup must have a path present for the path to be represented on the subgroup level map. In sum, the final solution from S-GIMME includes group-, subgroup-, and individual-level paths that are all estimated at the individual-level.

5.6. Inhibitory control

Inhibitory control was assessed on visit 6, following the fMRI scan. Children were offered a small snack (i.e., cheese crackers, grapes, and apple juice) between the fMRI and SST so that they were in a neutral appetitive state during the task. The stop signal task assesses inhibitory control by measuring the latency of response inhibition. The current version of the stop signal task used was developed specifically for this study to assess individual differences in children's inhibitory control in response to food images that varied by portion size (i.e., large versus small) and energy density (i.e., high calorie versus low calorie). However, in the current analyses, we focused only on children's overall performance (i.e., independent of the food condition they were responding to). The stop signal task was administered using Matlab2018b and Psychtoolbox3 (Kleiner et al., 2007). Pictures of plates of food were presented with a triangle folded napkin on either the left or right side of the plate (go-signal; see Fig. 1) for 1500 ms with an inter-stimulus-interval of 50 ms (i.e., fixation). Children were asked to sort the plates according to which side of the plate the napkin was on and to press the left or right arrow keys when the napkin appeared on the left or right side of the plate, respectively. They were encouraged to respond as quickly as possible. Children were also told that the plate would be sometimes get covered with a silver cloche (i.e., stop-signal; see Fig. 1) and were instructed not to respond if the silver cloche appeared. The silver cloche (i.e., stop-signal) was presented after variable delay on (25% of trials). The variable stop-signal delay (SSD) was determined by a step-wise adaptive procedure which increased the SSD 50 ms after each successful stop trial and reduced the SSD by 50 ms after each unsuccessful stop trial with the first SSD = 250 ms. This adaptive procedure maintained ~0.50 probability of successful response inhibition. The task parameters were based on specifications articulated by Verbruggen et al. (2019) for best practices in measuring stop-signal reaction time according to the theoretical racehorse model.

The task consisted of 256 trials across of 4 randomized blocks (i.e., 64 trials per block). After the practice, children were reminded to respond quickly and told that they may be encouraged to respond quickly during the task. To prevent children from slowing throughout the task, the message 'Faster' was presented after trials in which they responded slower than 1.5 standard deviations below their mean reaction time in practice. Between each block, children were given the opportunity to take a break and were shown their average response time (e. g., 'How Fast Were You?'), given encouragement for how quickly they were responding (e.g., 'Wow, that is faster than a second'), and were
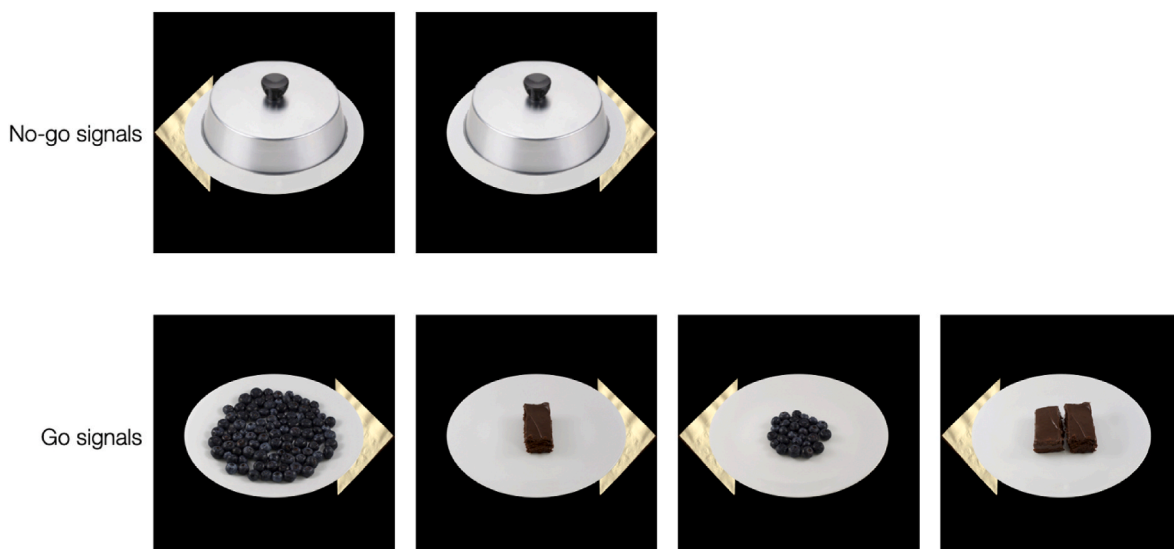

Fig. 1. Schematic depicting stop signal task.

reminded not to press the arrow keys if the silver cloche covered the plate.

Stop-signal reaction times (SSRT) were computed using the integration method after replacing omitted go responses with the participants' slowest go RT (Verbruggen et al., 2019). SSRT was only computed if the assumptions of the racehorse model were met (i.e., mean go RT > mean unsuccessful stop RT; Verbruggen et al., 2019). Of the 51 children who provided resting state data, 44 children provided SSRT data. Additionally, 1 participant's SSRT was excluded for not meeting the assumptions of the race model, and was therefore also treated as missing data.

5.7. Anxiety symptoms

Participants reported on their own anxiety symptoms using the Revised Children's Manifest Anxiety Scale (RCMAS), a 37-item questionnaire that asks children to endorse whether they do or do not experience a behavior (example: "I have trouble making up my mind"). Children filled out this questionnaire at their second laboratory visit. The RCMAS correlates highly with the trait anxiety subscale of the State-Trait Anxiety Inventory for children (STAIC), but not the state subscale, demonstrating construct validity with trait anxiety (Reynolds, 1980). The RCMAS is a reasonably stable measure of anxiety in school-age populations (Reynolds, 1981) and demonstrates good test-retest reliability (Wisniewski et al., 1987). We were interested in trait anxiety in contrast to state anxiety; it is the stable, persistent symptom profile that is of greater clinical relevance than ordinary intraindividual fluctuations in anxiety (Beauchaine, 2015).

For our analysis we used the total anxiety score of the RCMAS, which ranged from 0 to 28. Endorsing 19 or more behaviors (N = 6) indicates clinically significant levels of anxiety (Stallard et al., 2001). Forty five of the 51 children who provided useable resting state data also provided data from the RCMAS. Within our sample, this score had excellent internal consistency (Cronbach's Alpha = 0.89).

Additionally, we collected information on the child's level of state anxiety immediately before the fMRI using the Children's Anxiety Meter – State (CAMS-S; Ersig et al., 2013). For this measure, children are presented with a thermometer-like graphic and are asked to mark where they feel right now, with the bottom annotated as "Calm, not nervous or worried" and the top annotated as "Very very nervous or worried." The child's mark is then translated into a numeric value, with 0 representing lowest levels of state anxiety and 10 representing highest levels of state anxiety. Fifty of the 51 children providing resting state data also provided CAMS data.

5.8. Data analysis

All statistical analyses were conducted in R version 3.6.2. S-GIMME was used to generate data-driven subgroups characterizing resting state connectivity between regions of the PFC and the amygdala. In all analyses, familial obesity risk status ("high risk" if maternal BMI >30 kg/m^2 and paternal BMI >25 kg/m^2), age, and sex were treated as covariates. We also entered pre-scan state anxiety as a covariate in these models to control for the child's mental state upon entering the scanner (Ersig et al., 2013).

Using subgroup memberships derived from S-GIMME, we identified two connectivity groups of children: one with recovered connections between regions of the PFC and the amygdala, and one without these recovered connections. Then, we tested connectivity group differences in anxiety, as measured by the RCMAS, and in SSRT, as a metric of inhibitory control. Finally, we tested whether SSRT moderated the association between connectivity group membership and anxiety symptoms.

6. Results

S-GIMME identified five subgroups in the sample. The number of members in each subgroup can be found in Table 2.

To assess model fit for the final solution, we used recommendations published by Gates and Molenaar (2012). The average root mean squared error of approximation (RMSEA) was 0.10, the average standardized root mean–square residual (SRMR) was 0.04, the average non-normed fit index (NNFI) was 0.92, and the and the average comparative fit index (CFI) was 0.96. Because the SRMR <0.05 and CFI >0.95, we deemed the model fit excellent (Gates and Molenaar, 2012; Hu and Bentler, 1999).

Our hypotheses were central to functional connections between regions of the PFC and the amygdala, and we had no hypotheses specific to intra-region PFC connectivity or connections between more specific regions of the PFC and the amygdala. Therefore, we collapsed across subgroups that did (N = 2) and did not (N = 3) recover significant connections between regions of the PFC and the amygdala for analysis (Fig. 2). Thus, group membership was included in models as a dichotomous variable. For these final groups, group 1 (characterized by the presence of recovered connections between regions of the PFC and the amygdala) included 20 individuals, and group 2 (characterized by the absence of recovered connections between regions of the PFC and the amygdala) included 31 individuals. There were no significant differences in age, sex, familial risk for obesity, or head motion between these groups (all $p > .14$).

Analyses were conducted with all available data, so sample sizes varied slightly for each analysis as participants with fMRI data did not provide all behavioral data (Table 3). First, we assessed differences in anxiety and SSRT in the connectivity groups. Count of anxiety symptoms and their distribution, faceted by connectivity group, are plotted in Fig. 3. We statistically tested whether connectivity group membership was related to anxiety symptoms, while covarying for sex, age, pre-scan state anxiety, and obesity risk. In assessing relations to anxiety symptoms, we used a negative binomial distribution to account for the count-nature of the variable, as well as overdispersion within the sample (Cameron and Trivedi, 1990). There were no significant relations between connectivity group and number of reported anxiety symptoms. Results from the model can be seen in Table 3 (see Table 4).

Next, we tested whether connectivity group membership was related to SSRT, while covarying for sex, age, pre-scan state anxiety, and obesity risk. SSRT data and distribution, faceted by connectivity group, are plotted in Fig. 3. A normal distribution was used in this analysis. There was a significant negative association between connectivity group membership and SSRT, $b(SE) = -55.54(24.84)$, $p = .03$. That is, individuals characterized by no recovered connections between regions of the PFC and the amygdala (group 2) had faster SSRTs than individuals characterized by the presence of recovered connections between regions of the PFC and the amygdala (group 1). This pattern suggests better inhibitory control for members of group 2. Results from the model can be seen in Table 3.

We finally tested whether SSRT moderated the relation between connectivity group and anxiety symptoms, also using a negative binomial distribution. We found no significant interaction between SSRT and connectivity group, $b(SE) = 0.003(0.002)$, $p > .05$. However, we did find a significant conditional effect of SSRT on anxiety symptoms, $b(SE) =$

Table 2

Table displaying number of children in each S-GIMME generated subgroup.

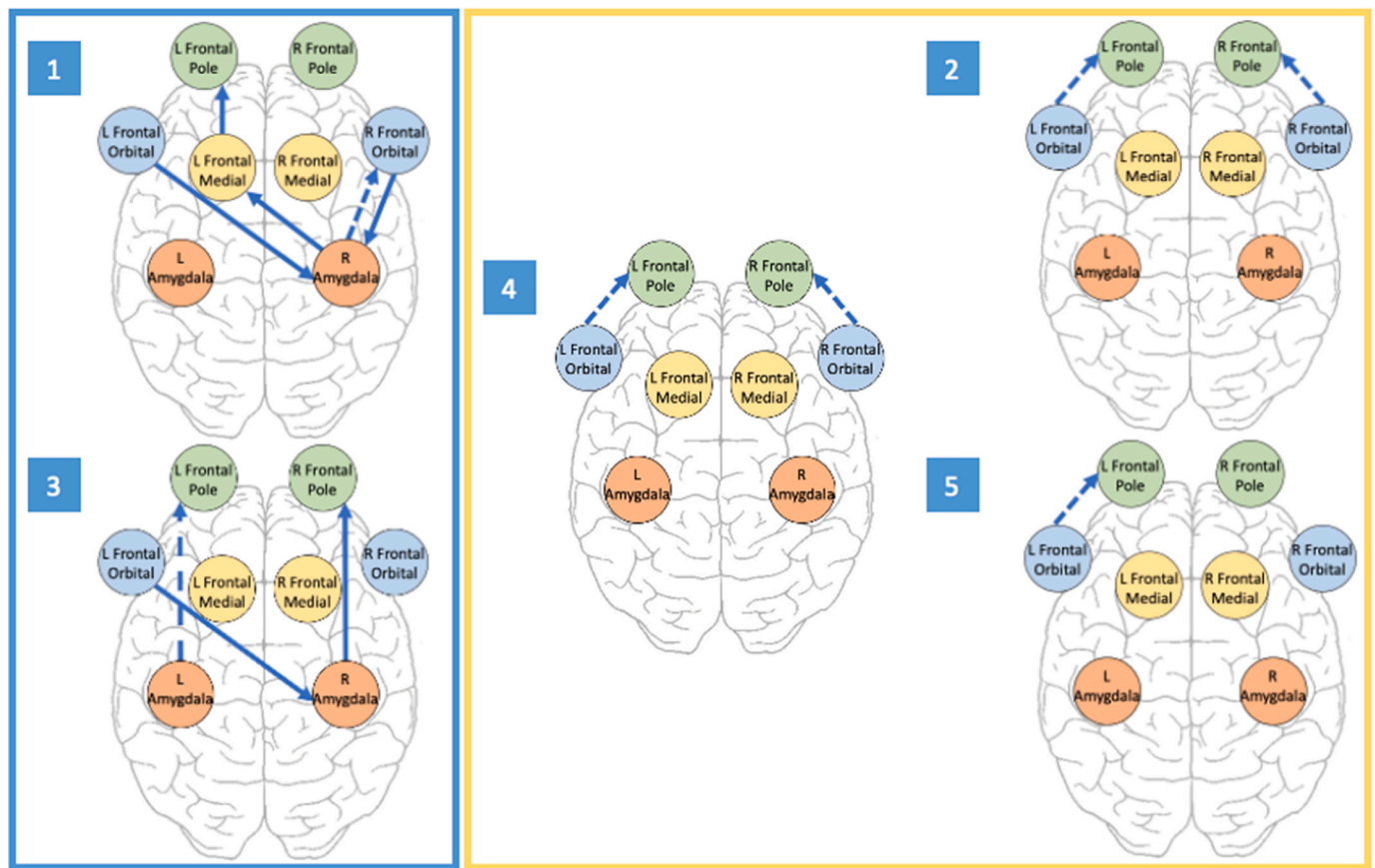| Subgroup	N	Final group
1	13	1
2	15	2
3	7	1
4	6	2
5	10	2

Fig. 2. Subgroups recovered by S-GIMME (N = 5). Only subgroup-level connections are shown; individual-level and group-level connections can be seen in the supplement (Fig. S1). Autoregressive effects are not depicted. Subgroups 2 and 4 are characterized by similar subgroup-level connections but are differentiated by individual-level connections, these are similarly depicted in the supplement. Solid lines represent contemporaneous effects and dashed lines represent lagged effects. Subgroups were collapsed to create two groups: 1) characterized by the recovery of significant connections between regions of the PFC and the amygdala (blue box) and 2) characterized by the absence of recovery of significant connections between regions of the PFC and the amygdala (yellow box). (For interpretation of the references to color in this figure legend, the reader is referred to the Web version of this article.)

Table 3
Negative binomial and linear models assessing relations between connectivity group and self-reported anxiety symptoms via the RCMAS and inhibitory control performance indexed by SSRT, respectively. Odds included for model ran using a negative binomial distribution. Sex, age, pre-scan state anxiety, and obesity risk category were entered as covariates in all models.

Parameter	Anxiety symptoms (RCMAS)				SSRT		
	N = 44				N = 42		
	Estimate	SE	Odds ratio	z-value	Estimate	SE	t-value
Intercept	1.44	1.40	4.22	1.02	1026.52***	166.10	6.18
Sex	−0.15	0.20	0.86	−0.77	−5.72	23.92	−0.24
Age	0.09	0.17	1.09	0.57	−82.69***	19.59	−4.22
Familial obesity risk status	0.23	0.19	1.26	1.20	58.42*	24.73	2.36
Pre-scan state anxiety	0.07	0.04	1.07	1.56	−7.12	4.97	−1.43
Connectivity group	−0.07	0.20	0.93	−0.32	−55.54*	24.84	−2.24

+$p < .10$, *$p < .05$, **$p < .01$, ***$p < .001$ Sex: 0 = female, 1 = male Familial obesity risk status: 0 = low risk, 1 = high risk Connectivity group: 1 = PFC-Amygdala connections recovered, 2 = PFC-Amygdala connections not recovered

−0.005(0.002), $p = .007$. A follow-up analysis found that while co-varying for group membership, there was a significant effect of SSRT on self-reported anxiety symptoms, $b = -0.002$, $p = .048$ (Table 5). That is, for a 10 ms increase in SSRT (indicating less proficient inhibitory control), the expected log count of the number of reported anxiety symptoms decreases by 0.03 or 3% (Odds Ratio for 10 ms increase = 0.97). The relation between SSRT and anxiety symptoms faceted by connectivity group is visualized in Fig. 4.

7. Discussion

In this study, we tested the interaction between inhibitory control performance and patterns of resting state PFC-amygdala connectivity in relation to anxiety symptoms. To do so, we used a data-driven approach to identify subgroups of children with unique patterns of PFC-amygdala resting state connectivity.

S-GIMME freely constructs subgroups without *a priori* specification of number of desired subgroups. Thus, the finding of five subgroups within this sample highlights the heterogeneity of patterns of PFC-
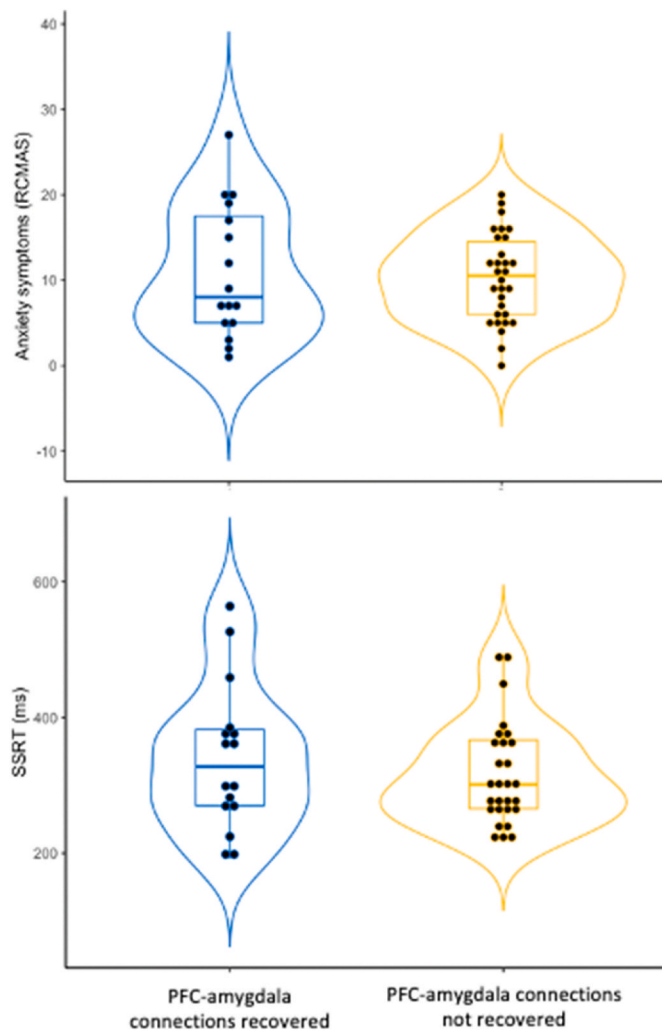
Fig. 3. Violin plot depicting the mean, range, and distribution of both SSRT and self-reported anxiety symptoms, split by connectivity group.

Table 4

Negative binomial model assessing the interaction between SSRT and connectivity group on self-reported anxiety symptoms. Sex, age, pre-scan state anxiety, and obesity risk category were entered as covariates.

Parameter	Estimate	SE	Odds ratio	z-value
Intercept	5.89**	2.15	361.41	2.73
Sex	−0.20	0.20	0.82	−1.02
Age	−0.25	0.21	0.78	−1.20
Familial obesity risk status	0.31	0.18	1.36	1.50
Pre-scan state anxiety	0.02	0.04	1.02	0.44
Connectivity group	−1.24+	0.72	0.29	−1.73
SSRT	−0.005**	0.002	0.995	−2.67
Connectivity group x SSRT	0.003	0.002	1.003	1.58

$+p < .10$, *$p < .05$, **$p < .01$, ***$p < .001$ Model based on 38 persons Sex: 0 = female, 1 = male Familial obesity risk status: 0 = low risk, 1 = high risk Connectivity group: 1 = PFC-Amygdala connections recovered, 2 = PFC-Amygdala connections not recovered.

amygdala connectivity in this developmental window, especially in a sample unselected for anxiety or anxiety risk. We also note that the majority of children within this sample (31 of 51) were assigned to the subgroups where significant connections between regions of the PFC and the amygdala were not recovered. Middle childhood is a period of significant change for both the PFC and its functional connections (Casey et al., 2005; Gee et al., 2013; Tottenham and Gabard-Durnam, 2017).

Table 5

Negative binomial model assessing the effect of SSRT on self-reported anxiety symptoms. Sex, age, pre-scan state anxiety, obesity risk category, and connectivity group were entered as covariates.

Parameter	Estimate	SE	Odds ratio	z-value
Intercept	4.70*	2.10	109.95	2.26
Sex	−0.19	0.20	0.83	−0.94
Age	−0.20	0.21	0.82	−0.93
Familial obesity risk status	0.34	0.21	1.40	1.59
Pre-scan state anxiety	0.04	0.04	1.04	0.81
Connectivity group	−0.16	0.23	0.85	−0.71
SSRT	−0.003*	0.001	0.997	−1.97

$+p < .10$, *$p < .05$, **$p < .01$, ***$p < .001$ Model based on 38 persons Sex: 0 = female, 1 = male Familial obesity risk status: 0 = low risk, 1 = high risk Connectivity group: 1 = PFC-Amygdala connections recovered, 2 = PFC-Amygdala connections not recovered.

The heterogeneity noted here may be capturing a period of large developmental change, or it may be highlighting heterogeneity in these circuits that persists through the lifespan. Future research should address this question empirically by conducting similar analyses on resting state data in either a cross sectional or longitudinal sample, focusing on the years surrounding age 10 where this purported shift in directionality of connectivity between the PFC and the amygdala takes place (Gee et al., 2013).

We collapsed across these five subgroups to yield two groups for analysis that were more central to our research question. Group one was characterized by individuals in the subgroups where S-GIMME recovered connections between regions of the PFC and the amygdala, while group two was characterized by individuals without PFC-amygdala connections. We tested whether these groups differed on their reported anxiety symptoms or inhibitory control performance. Children characterized by no recovered connections between regions of the PFC and the amygdala had more proficient inhibitory control than children who did show these connections. However, we found no significant association between connectivity group membership and child-reported anxiety symptoms. Of note, we used self-reported anxiety symptoms rather than parent-report, and future research may be strengthened by incorporating both child and parent report of anxiety symptoms. While future research should attempt replication in a larger sample to see if this relation is robust, the current association suggests that children for whom S-GIMME recovered connections between regions of the PFC and the amygdala may have *less* proficient inhibitory control, reflected in longer SSRTs. Meanwhile, we hypothesized that children with recovered connections between regions of the PFC and the amygdala would display faster SSRTs. Future work should address this association more directly, and in a larger sample, to examine potential mechanistic links between PFC-amygdala resting state connectivity and inhibitory control, and why these recovered connections may be associated with the longer SSRTs seen in this sample.

Finally, integrating SSRT, anxiety, and connectivity group membership into the same model, we found that greater SSRTs, reflecting less proficient inhibitory control, were related to fewer self-reported anxiety symptoms, but only when covarying for connectivity group. This finding is consistent with previous work suggesting that high levels of control may not always be adaptive for healthy development. Our findings regarding the interaction between connectivity and SSRT on anxiety were not entirely consistent with our hypothesis. We predicted that children not showing recovered connections between the PFC and amygdala would display higher levels of concurrent anxiety symptoms when they also had proficient inhibitory control. However, we found no significant interactions between connectivity group and inhibitory control. Rather, the positive association between SSRT and anxiety symptoms was present when *covarying* for connectivity group. While the relation between SSRT and anxiety is not moderated by connectivity, these findings show that trait-level regulatory mechanisms are
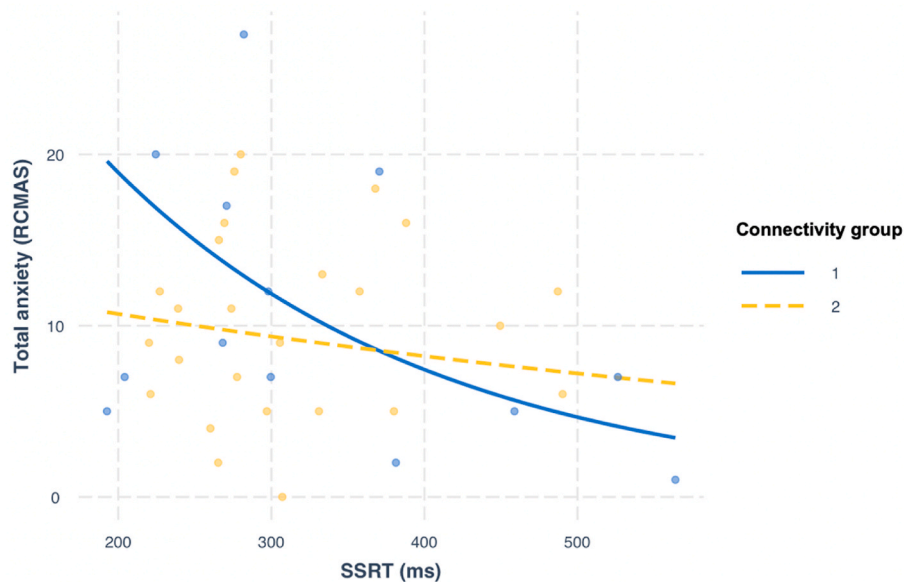
Fig. 4. Plot depicting negative effect of SSRT on self-reported anxiety symptoms, faceted by connectivity group membership.

important to consider when examining the relation between executive functioning and anxiety risk. This is in line with the idea that trait-level biopsychosocial factors, like temperament, may further explain the links between executive functioning and socioemotional processes (Henderson et al., 2015; Henderson and Wilson, 2017; White et al., 2011). The absence of a significant interaction in our model also suggests that high inhibitory control as a risk factor for internalizing behaviors may be a phenomenon that indeed holds true for the general population, which may have important implications for the framing of how inhibitory control is fostered in social and educational settings starting in childhood.

We also note that the absence of a significant interaction could be potentially attributed to sampling scheme. Our sample was recruited from the community and was not intentionally oversampled for over- or under-control. Indeed, the distribution of the SSRT metric for the sample was relatively normal (skewness = −.83, kurtosis = 3.13). Because children who were extremely over- or under-controlled were not strongly represented in this data set, it may have limited our ability to detect effects (Northoff and Tumati, 2019).

A relatively homogenous sample may have also influenced our findings. We recognize that this sample was not nationally representative, as children were majority white and high SES, as well as from highly educated families. Additionally, this sample was predominantly composed of children who were not clinically anxious. Only 6 of the 52 children reported clinically-relevant symptom levels. This may be due in part to the fact that while anxiety disorders may be diagnosed as young as preschool-age (Franz et al., 2013), onset of clinical-level symptomology may also be as late as adolescence or adulthood depending on the specific diagnosis (Beesdo et al., 2009). A slightly older sample or following children longitudinally may also offer more variability in anxiety symptoms.

We should interpret these findings based on a number of methodological considerations, including age-related differences in cognitive state while an individual is instructed to rest during a resting state scan. For example, for a younger child, resting state scans may elicit greater levels of cognitive control as they suppress a desire to move or talk during the scan. Network properties may reflect this heightened state of cognitive control. Inconsistencies in prior work may in part reflect the unstructured nature of a resting state scan, and findings should consider the fact that the actual "task" of laying still in a scanner may vary systematically across development (Camacho et al., 2020), as well as

individuals. Furthermore, we recognize that parcellation is an important methodological decision, especially in assessing resting state connectivity (Bryce et al., 2021), and these results are specific to anatomic brain regions defined by the Harvard-Oxford atlas. Our decision to use the Harvard-Oxford atlas was informed by prior work with similar research questions and samples (e.g., Liu et al., 2021), however different parcellations have the potential to yield different results than reported in this manuscript.

Additionally, while prior theoretical and empirical work suggests that the relation between inhibitory control and symptoms of anxiety may be nonlinear, we chose to model a linear relation. Quadratic modeling between variables relies on the assumption that individuals were not sampled along a normal distribution, with oversampling from individuals at the extremes of a bell curve. Because our sampling scheme did not consider this, we were not equipped to reliably model quadratic relations between variables. Future work should intentionally sample from low and high levels of both anxiety and inhibitory control to accurately assess quadratic relations between these constructs (Northoff and Tumati, 2019).

In conclusion, this study provides support of the notion that high levels of inhibitory control may relate to higher levels of self-reported anxiety symptoms as early as middle childhood. However, within this sample, these associations were evident when covarying for patterns of functional connections between the PFC and the amygdala. Thus, it may be important to consider neural circuitry *and* behavior in characterizing risk for anxiety within middle childhood.

Credit author statement

Kelley E. Gunther: Conceptualization, Methodology, Formal analysis, Writing – original draft **Daniel Petrie**: Methodology, Formal analysis, Writing – original draft **Alaina L. Pearce**: Writing – Review & Editing, Project administration **Bari A. Fuchs**: Writing – Review & Editing, Project administration **Koraly Pérez-Edgar**: Writing – Review & Editing **Kathleen L. Keller**: Writing – Review & Editing, Project administration, Funding acquisition **Charles Geier**: Methodology, Writing – review & editing, Project administration, Funding acquisition

Appendix A. Supplementary data

Supplementary data to this article can be found online at https://doi.

org/10.1016/j.neuropsychologia.2022.108313.

References

Abraham, A., Pedregosa, F., Eickenberg, M., Gervais, P., Mueller, A., Kossaifi, J., Gramfort, A., Thirion, B., Varoquaux, G., 2014. Machine learning for neuroimaging with scikit-learn. Front. Neuroinf. 8 https://doi.org/10.3389/fninf.2014.00014.

Adise, S., Geier, C.F., Roberts, N.J., White, C.N., Keller, K.L., 2018. Food or money? Children's brains respond differently to rewards regardless of weight status. Pediatr. Obes. 14 (2), e12469 https://doi.org/10.1111/ijpo.12469.

Adolphs, R., 2008. Fear, faces, and the human amygdala. Curr. Opin. Neurobiol. 18, 166–172. https://doi.org/10.1016/j.conb.2008.06.006.

Ansari, T.L., Derakshan, N., 2011. The neural correlates of impaired inhibitory control in anxiety. Neuropsychologia 49, 1146–1153. https://doi.org/10.1016/j.neuropsychologia.2011.01.019.

Avants, B.B., Epstein, C.L., Grossman, M., Gee, J.C., 2008. Symmetric diffeomorphic image registration with cross-correlation: evaluating automated labeling of elderly and neurodegenerative brain. Med. Image Anal. 12 (1), 26–41. https://doi.org/10.1016/j.media.2007.06.004.

Barkley, R.A., 1997. Behavioral inhibition, sustained attention, and executive functions: constructing a unifying theory of ADHD. Psychol. Bull. 121 (1), 65–94. https://doi.org/10.1037/0033-2909.121.1.65.

Basten, U., Stelzel, C., Fiebach, C.J., 2011. Trait anxiety modulates the neural efficiency of inhibitory control. J. Cognit. Neurosci. 23 (10), 3132–3145. https://doi.org/10.1162/jocn_a_00003.

Basten, U., Stelzel, C., Fiebach, C.J., 2012. Trait anxiety and the neural efficiency of manipulation in working memory. Cognit. Affect Behav. Neurosci. 12, 571–588. https://doi.org/10.3758/s13415-012-0100-3.

Baxter, A.J., Scott, K.M., Vos, T., Whiteford, H.A., 2013. Global prevalence of anxiety disorders: a systematic review and meta-regression. Psychol. Med. 43 (5), 897–910.

Beauchaine, T.P., 2015. Future directions in emotion dysregulation and youth psychopathology. J. Clin. Child Adolesc. Psychol. 45 (5), 875–896. https://doi.org/10.1080/15374416.2015.1038827.

Beesdo, K., Knappe, S., Pine, D.S., 2009. Anxiety and anxiety disorders in children and adolescents: developmental issues and implications for DSM-V. Psychiatr. Clin. 32 (3), 483–524. https://doi.org/10.1016/j.psc.2009.06.002.

Behzadi, Y., Restom, K., Liau, J., Liu, T.T., 2007. A component based noise correction method (CompCor) for BOLD and perfusion based fMRI. Neuroimage 37 (1), 90–101. https://doi.org/10.1016/j.neuroimage.2007.04.042.

Blackwell, K.A., Chatham, C.H., Wiseheart, M., Munakata, Y., 2014. A developmental window into trade-offs in executive function: the case of task switching versus response inhibition in 6-year-olds. Neuropsychologia 62, 356–364. https://doi.org/10.1016/j.neuropsychologia.2014.04.016.

Bora, E., Yucel, M., Pantelis, C., 2009. Cognitive endophenotypes of bipolar disorder: a meta-analysis of neuropsychological deficits in euthymic patients and their first-degree relatives. J. Affect. Disord. 113 (1–2), 1–20. https://doi.org/10.1016/j.jad.2008.06.009.

Bouwmeester, H., Smits, K., Van Ree, J.M., 2002a. Neonatal development of projections to the basolateral amygdala from prefrontal and thalamic structures in rat. J. Comp. Neurol. 450 (3), 241–255. https://doi.org/10.1002/cne.10321.

Bouwmeester, H., Wolterink, G., Van Ree, J.M., 2002b. Neonatal development of projections from the basolateral amygdala to prefrontal, striatal, and thalamic structures in the rat. J. Comp. Neurol. 442 (3), 239–249. https://doi.org/10.1002/cne.10084.

Brooker, R.J., Kiel, E.J., Buss, K.A., 2016. Early social fear predicts kindergarteners' socially anxious behaviors: direct associations, moderation by inhibitory control, and differences from nonsocial fear. Emotion 16 (7), 997–1010. https://doi.org/10.1037/emo0000135.

Bryce, N.V., Flournoy, J.C., Guassi Moreira, J.F., Rosen, M.L., Sambook, K.A., Mair, P., McLaughlin, K.A., 2021. Brain parcellation selection: an overlooked decision point with meaningful effects on individual differences in resting-state functional connectivity. Neuroimage 243, 118487. https://doi.org/10.1016/j.neuroimage.2021.118487.

Camacho, M.C., Quiñones-Camacho, L.E., Perlman, S.B., 2020. Does the child brain rest?: an examination and interpretation of resting cognition in developmental cognitive neuroscience. Neuroimage 212, 116688. https://doi.org/10.1016/j.neuroimage.2020.116688.

Cameron, A.C., Trivedi, P.K., 1990. Regression-based tests for overdispersion in the Poisson model. J. Econom. 46 (3), 347–364. https://doi.org/10.1016/0304-4076(90)90014-K.

Carlson, S.M., Moses, L.J., 2001. Individual differences in inhibitory control and children's theory of mind. Child Dev. 72 (4), 1032–1053. https://doi.org/10.1111/1467-8624.00333.

Carlson, S.M., Wang, T.A., 2007. Inhibitory control and emotion regulation in preschool children. Cognit. Dev. 22, 489–510. https://doi.org/10.1016/j.cogdev.2007.08.002.

Casey, B.J., Tottenham, N., Liston, C., Durston, S., 2005. Imaging the developing brain: what have we learned about cognitive development? Trends Cognit. Sci. 9 (3), 104–110. https://doi.org/10.1016/j.tics.2005.01.011.

Census Bureau, U.S., 2021. QuickFacts – Centre County, Pennsylvania. Retrieved from. https://www.census.gov/quickfacts/centrecountypennsylvania.

Cole, P.M., Deater-Deckard, K., 2009. Emotion regulation, risk, and psychopathology. JCPP (J. Child Psychol. Psychiatry) 50 (11), 1327–1330 https://doi.org/10.1111/j.1469-7610.2009.02180.x.

Cox, R.W., Hyde, J.S., 1997. Software tools for analysis and visualization of fMRI data. NMR Biomed. 10 (4–5), 171–178. https://doi.org/10.1002/(SICI)1099-1492(199706/08)10:4/5<171::AID-NBM453>3.0.CO;2-L.

Diamond, A., 2006. The early development of executive functions. In: Bialystok, E., Craik, F. (Eds.), Lifespan Cognition: Mechanisms of Change. Oxford University Press, New York, pp. 70–95.

Eggum-Wilkens, N.D., Reichenberg, R.E., Eisenberg, N., Spinard, T.L., 2016. Components of effortful control and their relations to children's shyness. IJBD (Int. J. Behav. Dev.) 40 (6), 544–554. https://doi.org/10.1177/0165025415597792.

English, L.K., Masterson, T.D., Fearnbach, S.N., Tanofsky-Kraff, M., Fisher, J., Wilson, S. J., Rolls, B.J., Kelley, K.L., 2019. Increased brain and behavioural susceptibility to portion size in children with loss of control eating. Pediatr. Obes. 14 (2) https://doi.org/10.1111/ijpo.12436.

Ersig, A.L., Kleiber, C., McCarthy, A.M., Hanrahan, K., 2013. Validation of a clinically useful measure of children's state anxiety before medical procedures. J. Spec. Pediatr. Nurs. (JSPN) 18 (4), 311–319. https://doi.org/10.1111/jspn.12042.

Esteban, O., Markiewicz, C., Goncalves, M., DuPre, E., Kent, J.D., Salo, T., Ciric, R., Pinsard, B., Blair, R.W., Poldrack, R.A., Gorgolewski, K.J., 2018a. FMRIPrep. *Software.* Zenodo. https://doi.org/10.5281/zenodo.852659.

Esteban, O., Markiewicz, C., Blair, R.W., Moodie, C., Isik, A.I., Erramuzpe, A., Kent, J., Goncalves, M., DuPre, E., Snyder, M., Oya, H., Ghosh, S.S., Wright, J., Durnezm, J., Poldrack, R.A., Gorgolewski, K.J., 2018b. fMRIPrep: a robust preprocessing pipeline for functional MRI. Nat. Methods 16, 111–116. https://doi.org/10.1038/s41592-018-0235-4.

Fitzpatrick, C., McKinnon, R.D., Blair, C.B., Willoughby, M.T., 2014. Do preschool executive function skills explain the school readiness gap between advantaged and disadvantaged children? Learning and Instruction 30, 25–31. https://doi.org/10.1016/j.learninstruc.2013.11.003.

Fonov, V.S., Evans, A.C., McKinstry, R.C., Almli, C.R., Collins, D.L., 2009. Unbiased nonlinear average age-appropriate brain templates from birth to adulthood. Neuroimage 47 (Suppl. 1), S102. https://doi.org/10.1016/S1053-8119(09)70884-5.

Franz, L., Angold, A., Copeland, W., Costello, E.J., Towe-Goodman, N., Egger, H., 2013. Preschool anxiety disorders in pediatric primary care: prevalence and comorbidity. J. Am. Acad. Child Adolesc. Psychiatr. 52 (12), 1294–1303. https://doi.org/10.1016/j.jaac/2013.09.008.

Gabard-Durnam, L.J., O'Muircheartaigh, J., Dirks, H., Dean III, D.C., Tottenham, N., Deoni, S., 2018. Human amygdala functional network development: a cross-sectional study from 3 months to 5 years of age. Developmental cognitive neuroscience 34, 63–74. https://doi.org/10.1016/j.dcn.2018.06.004.

Gates, K.M., Molenaar, P.C.M., 2012. Group search algorithm recovers effective connectivity maps for individuals in homogenous and heterogenous samples. Neuroimage 63, 310–319. https://doi.org/10.1016/j.neuroimage.2012.06.026.

Gates, K.M., Molenaar, P.C., Hillary, F.G., Ram, N., Rovine, M.J., 2010. Automatic search for fMRI connectivity mapping: an alternative to Granger causality testing using formal equivalences among SEM path modeling, VAR, and unified SEM. Neuroimage 50 (3), 1118–1125. https://doi.org/10.1016/j.neuroimage.2009.12.117.

Gates, K.M., Molenaar, P.C.M., Iyer, S.P., Nigg, J.T., Fairm, D.A., 2014. Organizing heterogeneous samples using community detection of GIMME-derived resting state functional networks. PLoS One 9 (3), e91322. https://doi.org/10.1371/journal.pone.0091322.

Gates, K.M., Lane, S.T., Varangis, E., Giovanello, K., Guiskewicz, K., 2017. Unsupervised classification during time-series model building. Multivariate Behav. Res. 52 (2), 129–148. https://doi.org/10.1080/00273171.2016.1256187.

Gates, K.M., Fisher, Z., Bollen, K.A., 2021. Latent variable GIMME. Psychol. Methods 25 (2), 227–242. https://doi.org/10.1037/met0000229.

Gee, D.G., Humphreys, K.L., Flannery, J., Goff, B., Telzer, E.H., Shapiro, M., Hare, T.A., Bookheimer, S.Y., Tottenham, N., 2013. A developmental shift from positive to negative connectivity in human amygdala-prefrontal circuitry. J. Neurosci. 33 (10), 4584–4593. https://doi.org/10.1523/JNEUROSCI.3446-12.2013.

Geiger, M.J., Domschke, K., Ipser, J., Hattingh, C., Baldwin, D.S., Lochner, C., Stein, D.J., 2016. Altered executive control network resting-state connectivity in social anxiety disorder. World J. Biol. Psychiatr. 17 (1), 47–57. https://doi.org/10.3109/15622975.2015.1083613.

Gorgolewski, K., Burns, C.D., Madison, C., Clark, D., Halchenko, Y.O., Waskom, M.L., Ghosh, S., 2011. Nipype: a flexible, lightweight and extensible neuroimaging data processing framework in Python. Front. Neuroinf. 5 (13) https://doi.org/10.3389/fninf.2011.00013.

Granger, C.W., 1969. Investigating causal relations by econometric models and cross-spectral methods. Econometrica: J. Econom. Soc. 424–438.

Graziano, P.A., Reavis, R.D., Keane, S.P., Calkins, S.D., 2007. The role of emotion regulation in children's early academic success. J. Sch. Psychol. 45 (1), 3–19. https://doi.org/10.1016/j.jsp.2006.09.002.

Greve, D.N., Fischl, B., 2009. Accurate and robust brain image alignment using boundary-based registration. Neuroimage 48 (1), 63–72. https://doi.org/10.1016/j.neuroimage.2009.06.060.

Gunther, K.E., Pérez-Edgar, K., 2021. Dopaminergic associations between behavioral inhibition, executive functioning, and anxiety in development. Dev. Rev. 60, 100966 https://doi.org/10.1016/j.dr.2021.100966.

Hahn, A., Stein, P., Windischberger, C., Weissenbacher, A., Spindelegger, C., Moser, E., Kasper, S., Lanxenberger, R., 2011. Reduced resting-state functional connectivity between amygdala and orbitofrontal cortex in social anxiety disorder. Neuroimage 56, 881–889 https://doi.org/10.1016/j.neuroimage.2011.02.041.

Henderson, H.A., Wilson, M.J.G., 2017. Attention processes underlying risk and resilience in behaviorally inhibited children. Current Behavioral Neuroscience Reports 4, 99–106. https://doi.org/10.1007/s40473-017-0111-z.

Henderson, H.A., Pine, D.S., Fox, N.A., 2015. Behavioral inhibition and developmental risk: a dual-processing perspective. Neuropsychopharmacology 40, 207–224 https://doi.org/10.1038.npp.2014.189.

Hoffman, D.L., Dukes, E.M., Wittchen, H.U., 2008. Human and economic burden of generalized anxiety disorder. Depress. Anxiety 25 (1), 72–90. https://doi.org/10.1002/da.20257.

Hu, L.T., Bentler, P.M., 1999. Cutoff criteria for fit indexes in covariance structure analysis: conventional criteria versus new alternatives. Struct. Equ. Model.: A Multidiscip. J. 6 (1), 1–55. https://doi.org/10.1080/10705519909540118.

Huntenburg, J.M., 2014. Evaluating nonlinear coregistration of BOLD EPI and T1w images. In: Master's Thesis. Freie Universität, Berlin. http://hdl.handle.net/11858/00-001M-0000-002B-1CB5-A.

Jenkinson, M., Smith, S., 2001. A global optimisation method for robust affine registration of brain images. Med. Image Anal. 5 (2), 143–156. https://doi.org/10.1016/S1361-8415(01)00036-6.

Jenkinson, M., Bannister, P., Brady, M., Smith, S., 2002. Improved optimization for the robust and accurate linear registration and motion correction of brain images. Neuroimage 17 (2), 825–841. https://doi.org/10.1006/nimg.2002.1132.

Keller, K.L., Assur, S.A., Torres, M., Lofink, H.E., Thornton, J.C., Faith, M.S., Kissileff, H. R., 2006. Potential of an analog scaling device for measuring fullness in children: development and preliminary testing. Appetite 47 (2), 233–243. https://doi.org/10.1016/j.appet.2006.04.004.

Kim, J., Zhu, W., Chang, L., Bentler, P.M., Ernst, T., 2007. Unified structural equation modeling approach for the analysis of multisubject, multivariate functional MRI data. Hum. Brain Mapp. 28 (2), 85–93. https://doi.org/10.1002/hbm.20259.

Kleiner, M., Brainard, D., Pelli, D., 2007. In: What's New in Psychtoolbox-3?.

Kooijmans, R., Scheres, A., Oosterlaan, J., 2000. Response inhibition and measures of psychopathology: a dimensional analysis. Child Neuropsychol. 6 (3), 145–184. https://doi.org/10.1076/chin.6.3.175.3154.

Lanczos, C., 1964. Evaluation of noisy data. J. Soc. Ind. Appl. Math. B Numer. Anal. 1 (1), 76–85. https://doi.org/10.1137/0701007.

Lane, S.T., Gates, K.M., 2017. Automated selection of robust individual-level structural equation models for time series data. Struct. Equ. Model.: A Multidiscip. J. 24 (5), 768–782. https://doi.org/10.1080/10705511.2017.1309978.

Lejuez, C.W., Read, J.P., Kahler, C.W., Richards, J.B., Ramsey, S.E., Stuart, G.L., et al., 2002. Evaluation of a behavioral measure of risk taking: the Balloon Analogue risk task (BART). J. Exp. Psychol. Appl. 8 (2), 75. https://doi.org/10.1037/1076-898X.8.2.75.

Lengua, L.J., 2003. Associations among emotionality, self-regulation, adjustment problems, and positive adjustment in middle childhood. Appl. Dev. Psychol. 24, 595–618. https://doi.org/10.1016/j.appdev.2003.08.002.

Liu, W.J., Yin, D.Z., Cheng, W.H., Fan, M.X., You, M.N., Men, W.W., Zang, L.L., Shi, D.H., Zhang, F., 2015. Abnormal functional connectivity of the amygdala-based network in resting-state fMRI in adolescents with generalized anxiety disorder. Med. Sci. Mon. Int. Med. J. Exp. Clin. Res.: Int. Med. J. Int. Med. J.Exp. Clin. Res. 21, 459–467. https://doi.org/10.12659/MSM.893373.

Liu, P., Vandermeer, M.R.J., Ali, O.M., Daoust, A.R., Joanisse, M.F., Barch, D.M., Hayden, E.P., 2021. Maternal Depression, Child Temperament, and Early-Life Stress Predict Never-Depressed Preadolescents' Functional Connectivity during a Negative-Mood Induction. Clinical Psychological Science. https://doi.org/10.1177/21677026211016419.

Lv, H., Wang, Z., Tong, E., Williams, L.M., Zaharchuk, G., Zeineh, M., Goldstein-Piekarski, A.N., Ball, T.M., Liao, C., Wintermark, M., 2018. Resting-state functional MRI: everything that nonexperts have always wanted to know. Am. J. Neuroradiol. 39 (8), 1390–1399. https://doi.org/10.3174/ajnr.A5527.

Lydon-Staley, D.M., Ciric, R., Satterthwaite, T.D., Bassett, D.S., 2019. Evaluation of confound regression strategies for the mitigation of micromovement artifact in studies of dynamic resting-state functional connectivity and multilayer network modularity. Network neuroscience 3 (2), 427–454. https://doi.org/10.1162/netn_a_00071.

Marek, S., Tervo-Clemmens, B., Calabro, F.J., Montez, D.F., Kay, B.P., Hatoum, A.S., Donohue, M.R., Foran, W., Miller, R.L., Hendrickson, T.J., Malone, S.M., Kandala, S., Feczko, E., Miranda-Dominguez, O., Graham, A.M., Earl, E.A., Perrone, A.J., Cordova, M., Doyle, O., Moore, L.A., Conan, G.M., Uriarte, J., Sniger, K., Lynch, B.J., Wilgenbusch, J.C., Pengo, T., Tam, A., Chen, J., Newbold, D.J., Zheng, A., Seider, N. A., Van, A.N., Metoki, A., Chauvin, R.J., Laumann, T.O., Greene, D.J., Petersen, S.E., Garavan, H., Thompson, W.K., Nichols, T.E., Yeo, B.T.T., Barch, D.M., Luna, B., Fair, D.A., Dosenbach, N.U., 2022. Reproducible brain-wide association studies require thousands of individuals. Nature 603, 654–660. https://doi.org/10.1038/s41586-022-04492-9.

McCormick, E.M., Gates, K.M., Telzer, E.H., 2019. Model-based network discovery of developmental and performance-related differences during risky decision-making. Neuroimage 188, 456–464. https://doi.org/10.1016/j.neuroimage.2018.12.042.

Miller, E.K., Cohen, J.D., 2001. An integrative theory of prefrontal cortex function. Annu. Rev. Neurosci. 24, 167–202.

Miyake, A., Friedman, N.P., Emerson, M.J., Witzki, A.H., Howerter, A., Wager, T.D., 2000. The unity and diversity of executive functions and their contributions to complex "frontal lobe" tasks: a latent variable analysis. Cognit. Psychol. 41 (1), 49–100. https://doi.org/10.1006/cogp.1999.0734.

Molenaar, P.C., 2004. A manifesto on psychology as idiographic science: bringing the person back into scientific psychology, this time forever. Measurement 2 (4), 201–218. https://doi.org/10.1207/s15366359mea0204_1.

Molenaar, P.C., Campbell, C.G., 2009. The new person-specific paradigm in psychology. Curr. Dir. Psychol. Sci. 18 (2), 112–117. https://doi.org/10.1111/j.1467-8721.2009.01619.x.

Moran, T.P., 2016. Anxiety and working memory capacity: a meta-analysis and narrative review. Psychol. Bull. 142 (8), 1–34. https://doi.org/10.1037/bul0000051.

Northoff, G., Tumati, S., 2019. Average is good, extremes are bad" - non-linear inverted U-shaped relationship between neural mechanisms and functionality of mental features. Neurosci. Biobehav. Rev. 104, 11–25. https://doi.org/10.1016/j.neubiorev.2019.06.030.

Ochsner, K.N., Silvers, J.A., Buhle, J.T., 2012. Functional imaging studies of emotion regulation: a synthetic review and evolving model of the cognitive control of emotion. Ann. N. Y. Acad. Sci. 1251, E1–E24. https://doi.org/10.1111/j.1749-6632.2012.06751.x.

Pérez-Edgar, K., Vallorani, A., Buss, K.A., LoBue, V., 2020. Individual differences in infancy research: letting the baby stand out from the crowd. Infancy 25, 438–457. https://doi.org/10.1111/infa.12338.

Pons, P., Latapy, M., 2006. Computing communities in large networks using random walks. J. Graph Algorithm Appl. 10 (2), 191–218.

Power, J.D., Mitra, A., Laumann, T.O., Snyder, A.Z., Schlaggar, B.L., Petersen, S.E., 2014. Methods to detect, characterize, and remove motion artifact in resting state fMRI. Neuroimage 84 (Suppl. C), 320–341. https://doi.org/10.1016/j.neuroimage.2013.08.048.

Prater, K.E., Hosanagar, A., Klumpp, H., Angstadt, M., Luan Phan, K., 2013. Aberrant amygdala–frontal cortex connectivity during perception of fearful faces and at rest in generalized social anxiety disorder. Depress. Anxiety 30 (3), 234–241. https://doi.org/10.1002/da.22014.

Reynolds, C.R., 1980. Concurrent validity of what I think and feel: the revised children's manifest anxiety scale. J. Consult. Clin. Psychol. 48 (6), 774–775. https://doi.org/10.1037/0022-006X.48.6.774.

Reynolds, C.R., 1981. Long-term stability of scores on the revised-children's manifest anxiety scale. Percept. Mot. Skills 53 (3), 702. https://doi.org/10.2466/pms.1981.53.3.702.

Rodrigues, E.R., Hassan, R., Schmidt, L.A., 2021. Negative Emotionality and Internalizing Behaviors in Preschool Children: Moderating Role of Inhibitory Control. Child Psychiatry & Human Development, pp. 1–9.

Satterthwaite, T.D., Elliott, M.A., Gerraty, R.T., Ruparel, K., loughead, J., Calkins, M.E., Eikhoff, S.B., Hakonarson, H., Gur, R.C., Gur, R.E., Wolf, D.H., 2013. An improved framework for confound regression and filtering for control of motion artifact in the preprocessing of resting-state functional connectivity data. Neuroimage 64, 240–256. https://doi.org/10.1016/j.neuroimage.2012.08.052.

Saygin, Z.M., Osher, D.E., Koldewyn, K., Martin, R.E., Finn, A., Saxe, R., Gabrieli, J.D.E., Sheridan, M., 2015. Structural connectivity of the developing human amygdala. PLoS One 10 (4), e0125170. https://doi.org/10.1371/journal.pone.0125170.

Shin, N.Y., Lee, T.Y., Kim, E., Kwon, J.S., 2014. Cognitive functioning in obsessive-compulsive disorder: a meta-analysis. Psychol. Med. 44 (6), 1121–1130. https://doi.org/10.1017/S0033291713001803.

Smith, S.M., Miller, K.L., Salimi-Khorshidi, G., Webster, M., Beckmann, C.F., Nichols, T. E., Ramsey, J.D., Woolrich, M.W., 2011. Network modeling methods for FMRI. Neuroimage 54 (2), 875–891. https://doi.org/10.1016/j.neuroimage.2010.08.063.

Snyder, H.R., Miyake, A., Hankin, B.L., 2015. Advancing understanding of executive function impairments and psychopathology: bridging the gap between clinical and cognitive approaches. Front. Psychol. 6 (328), 1–24. https://doi.org/10.3389/fpsyg.2015.00328.

Sörbom, D., 1989. Model modification. Psychometrika 54 (3), 371–384. https://doi.org/10.1007/BF02294623.

Stallard, P., Velleman, R., Langsford, J., Baldwin, S., 2001. Coping and psychological distress in children involved in road traffic accidents. Br. J. Clin. Psychol. 40 (2), 197–208.

Taber-Thomas, B., Pérez-Edgar, K., 2015. Brain development in emerging adulthood. In: Arnett, J. (Ed.), Oxford Handbook of Emerging Adulthood. Oxford University Press, pp. 126–141.

Thorell, L.B., Bohlin, G., Rydell, A., 2004. Two types of inhibitory control: predictive relations to social functioning. IJBD (Int. J. Behav. Dev.) 28 (3), 193–203. https://doi.org/10.1080/01650250344000389.

Toren, P., Sadeh, M., Wolmer, L., Eldar, S., Koren, S., Weizman, R., Laor, N., 2000. Neurocognitive correlates of anxiety disorders in children: a preliminary report. J. Anxiety Disord. 14 (3), 239–247. https://doi.org/10.1016/s0887-6185(99)00036-5.

Tottenham, N., Gabard-Durnam, L.J., 2017. The developing amygdala: a student of the world and a teacher of the cortex. Current Opinion in Psychology 17, 55–60. https://doi.org/10.1016/j.copsyc.2017.06.012.

Treiber, J.M., White, N.S., Steed, T.C., Bartsch, H., Holland, D., Farid, N., McDonald, C. R., Carter, B.S., Dale, A.M., Chen, C.C., 2016. Characterization and correction of geometric distortions in 814 diffusion weighted images. PLoS One 11 (3), e0152472. https://doi.org/10.1371/journal.pone.0152472.

Tustison, N.J., Avants, B.B., Cook, P.A., Zheng, Y., Egan, A., Yushkevich, P.A., Gee, J.C., 2010. N4ITK: improved N3 bias correction. IEEE Trans. Med. Imag. 29 (6), 1310–1320. https://doi.org/10.1109/TMI.2010.2046908.

Uddin, L.Q., Supekar, K., Menon, V., 2010. Typical and atypical development of functional human brain networks: insights from resting-state functional MRI. Front. Syst. Neurosci. 4, 21. https://doi.org/10.3389/fnsys.2010.00021.

Vanderwal, T., Kelly, C., Eilbott, J., Mayes, L.C., Castellanos, F.X., 2015. Inscapes: a movie paradigm to improve compliance in functional magnetic resonance imaging. Neuroimage 122, 222–232. https://doi.org/10.1016/j.neuroimage.2015.07.069.

Verbruggen, F., Aron, A.R., Band, G.P.H., Beste, C., Bissett, P.G., Brockett, A.T., Brown, J. W., Chamberlain, S.R., Chambers, C.D., Colonius, H., Colzato, L.S., Corneil, B.D., Coxon, J.P., Dupuis, A., Eagle, D.M., Garavan, H., Greenhouse, I., Heathcode, A., Huster, R.J., Jahfari, S., Kenemans, J.L., Leunissen, I., Li, C.R., Logan, G.D., Matzke, D., Morein-Zamir, S., Murthy, A., Paré, M., Poldrack, R.A., Ridderinkhof, K.

R., Robbins, T.W., Roesch, M., Rubia, K., Schacher, R.J., Schall, J.D., Stock, A., Swann, N.C., Thakkar, K.N., van der Molen, M.W., Vermeylen, L., Vink, M., Wessel, J.R., Whelan, R., Zandbelt, B.B., Boehler, C.N., 2019. A consensus guide to capturing the ability to inhibit actions and impulsive behaviors in the stop-signal task. Elife 8, e46323. https://doi.org/10.7554/eLife.46323.

Wang, S., Peterson, D.J., Gatenby, J.C., Li, W., Grabowski, T.J., Madhyastha, T.M., 2017. Evaluation of field map and nonlinear registration methods for correction of susceptibility artifacts in diffusion MRI. Front. Neuroinf. 11 https://doi.org/10.3389/fninf.2017.00017.

Welsh, M.C., Pennington, B.F., Groisser, D.B., 1991. A normative-developmental study of executive function: a window on prefrontal function in children. Dev. Neuropsychol. 7 (2), 131–149. https://doi.org/10.1080/87565649109540483.

White, L.K., McDermott, J.M., Degnan, K.A., Henderson, H.A., Fox, N.A., 2011. Behavioral Inhibition and anxiety: the moderating roles of inhibitory control and attention shifting. J. Abnorm. Child Psychol. 39, 735–747. https://doi.org/10.1007/s10802-011-9490-x.

Wisniewski, J.J., Genshaft, J.L., Mulick, J.A., Coury, D.L., 1987. Test-retest reliability of the revised children's manifest anxiety scale. Percept. Mot. Skills 65 (1), 67–70.

Wittchen, H.U., 2002. Generalized anxiety disorder: prevalence, burden, and cost to society. Depress. Anxiety 16 (4), 162–171. https://doi.org/10.1002/da.10065.

Wolfe, C.D., Bell, M.A., 2014. Brain electrical activity of shy and non-shy preschool-aged children during executive function tasks. Infant Child Dev. 23 (3), 259–272. https://doi.org/10.1002/icd.1858.

Zelazo, P.D., 2020. Executive function and psychopathology: a neurodevelopmental perspective. Annu. Rev. Clin. Psychol. 16, 431–454. https://doi.org/10.1146/annurev-clinpsy-072319-024242.

Zelazo, P.D., Carlson, S.M., Kesek, A., 2008. The development of executive function in childhood. In: Nelson, C.A., Luciana, M. (Eds.), Developmental Cognitive Neuroscience. Handbook of Developmental Cognitive Neuroscience. MIT Press, pp. 553–574.

Zhang, Y., Brady, M., Smith, S., 2001. Segmentation of brain MR images through a hidden markov random field model and the expectation-maximization algorithm. IEEE Trans. Med. Imag. 20 (1), 45–57. https://doi.org/10.1109/42.906424.